Radiophysics and Quantum Electronics, Vol. 47, No. 3, 2004

DETERMINATION OF THE PARAMETERS OF SEA-SURFACE ROUGHNESS USING THE DOPPLER SPECTRUM OF A MICROWAVE RADAR SIGNAL REFLECTED FROM A WATER SURFACE

E. M. Meshkov * **and V. Yu. Karaev**

UDC 621.371.165

Within the framework of the Kirchhoff approximation, we derive formulas describing the shift and width of the Doppler spectrum of a microwave signal reflected from a rough water surface in the case of a small incidence angle. The formulas take into account the effect of the radar beam pattern. The new model of the spectrum allows for the fact that the distance from the radar to the observed surface changes in the course of measurements. Our theoretical analysis shows that the Doppler-spectrum parameters and the amount of information on the scattering surface, which is contained in the reflected signal, are strongly dependent on the antenna beamwidth. The results of our study allowed us to develop a new algorithm for measuring the water-surface parameters from a moving carrier.

1. INTRODUCTION

Development of the methods of radar sensing of the oceanic surface is necessary for solution of many applied problems such as, for example, life security in the coastal areas, ecological monitoring of the ocean, and collecting meteorological information. Modern radars permit one to measure different characteristics of the sea surface, for example, the roughness height and the velocity and direction of wind. At present, retrieval of the scattering-surface parameters is based on analyzing the reflected-signal power (backscattering cross section).

In the present paper, we consider the problem of increasing the number of sea-surface characteristics, measurable by remote methods, due to analysis of the reflected-signal spectrum. As is shown below, the variance in water-surface slopes can be measured with high accuracy.

Another, no less important problem is to improve the accuracy of measurement of the retrieved parameters, for example, the wind velocity, due to obtaining additional information on the state of the scattering surface.

What are the reasons for the errors of measurement of the wind velocity and what are the ways to eliminate them? The currently used techniques for wind-velocity retrieval involve regression algorithms based on the assumption that the relationship between the backscattering and the wind velocity is single-valued [1–4]. However, the relationship between the reflected-signal power and the wind velocity is not single-valued, i. e., the parameters of large-scale roughness are not always related to only the wind velocity. The scattering cross section depends on the variance of water-surface slopes and the spectral density of the ripples. Hence, the accurate determination of the wind velocity requires knowledge of the variance of large-scale roughness slopes.

* meshkov@hydro.appl.sci-nnov.ru

Institute of Applied Physics of the Russian Academy of Sciences, Nizhny Novgorod, Russia. Translated from Izvestiya Vysshikh Uchebnykh Zavedenii, Radiofizika, Vol. 47, No. 3, pp. 231–244, March, 2004. Original article submitted April 18, 2003.

0033-8443/04/4703-0205

Gravity-capillary waves correlate well with the wind velocity, while the characteristics of large-scale roughness depend not only on the wind, but also on the presence of ripple waves and the degree of roughness development. Hence, the error of retrieval of the wind velocity is maximum under conditions of weak wind and high ripples [5].

Methods for measurement of the surface-slope variance exist [6, 7], but they have constraints. For example, the SRA altimeter [6] makes it possible to measure surface slopes, but the method used in it is limited by the fact that measurements should be conducted from a moderate height since the size of a cell (resolution element) must be much smaller than the wavelength of the energy-carrying sea-surface roughness. Therefore, this method cannot be applied for satellite-borne measurements.

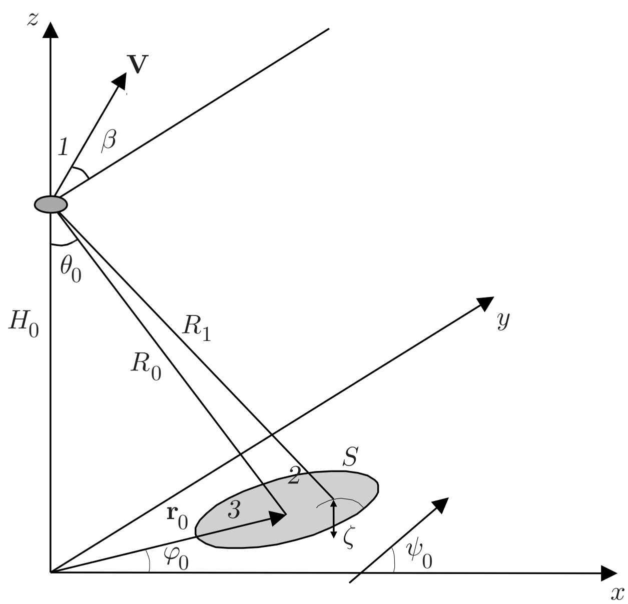

Fig. 1.

The present paper is devoted to a study of spectral characteristics of a reflected microwave signal (Doppler spectrum) as a basis for the development of new methods and algorithms for determining scattering-surface parameters.

The initial period of study of the Doppler spectrum is referred to the second half of the fifties. It was exactly the Doppler measurements in the decameter wavelength range [8–10] that were the basis on which an adequate concept of the mechanism of scattering of HF radio waves by a sea surface was formulated for the first time. Then the corresponding theory was extended to the microwave range [11, 12]. Later on, the main effort was focused on a study of the backscattering cross section and its use for obtaining information on the sea surface (see, e. g., [1–4]).

Within the framework of the Kirchhoff method, we obtained formulas for the shift and width of the Doppler spectrum (DS) of electromagnetic waves of the microwave range scattered by a rough water surface at small incidence angles with allowance for the beam pattern (BP) of the radar [13]. As is well known, not only an airplane cannot move rigorously parallel to the sounded surface, but also a satellite moves only along an orbit of variable radius. Hence, to make the DS model usable for the interpretation of field-measurement data, we introduced an inclination angle between the trajectory of motion in the vertical plane and the horizontal axis. This angle describes variations in the radar height with respect to the sea surface and is not related to the incidence angle. A change in the inclination angle does not lead to a change in the incidence angle. In the present paper, we obtain formulas for the width and shift of the DS and estimate the efficiency of the algorithms of retrieval of information on the sea-surface state.

2. FORMULATION OF THE PROBLEM

Consider the formulation of the initial problem. Figure 1 shows the scheme of measurements. The radar moves in the yz plane, its velocity $\mathbf{V}$ is assumed constant, β is the inclination angle between the velocity vector and the y axis. Observation is performed at an incidence angle θ_0, which is assumed fairly small, such that the backscattering mechanism of a radar microwave signal is quasi-mirror, and account of the Bragg component is unnecessary. The direction of propagation of the sea-surface roughness is determined by the angle ψ_0, which, as also the antenna slewing angle φ_0, is reckoned from the x axis.

The beam pattern $G(\mathbf{r})$ is assumed Gaussian (see the text below) and has the half-power beamwidth δ_x in the vertical plane and δ_y in the azimuthal plane. The oblique distance to the scattering-area center is $R_0 = H_0/\cos\theta_0$. The current point on the scattering area has the coordinates (x_1, y_1, ζ_1), where $\zeta_1(\mathbf{r}, t)$ is a random function describing large-scale roughness, R_1 is the corresponding oblique distance to the reflection point, and $\mathbf{r}_0(x_0, y_0)$ is the radius vector to the center of the scattering area S in the xy plane.

Within the Kirchhoff-method approximation, the complex amplitude of the scattered field of a quasi-mirror component has the following form [14–17]:

$$E_{\mathrm{m}}(t)=\frac{F_{\mathrm{eff}}(U_{10})E_0k}{2\pi i\cos\theta_0 R_0}\int\limits_S G(\mathbf{r})\exp(-2ikR_1)\,\mathrm{d}S, \tag{1}$$

where E_0 is the amplitude of the incident field near the scattering surface, U_{10} is the wind velocity at the height 10 m above the surface, $F_{\mathrm{eff}}(U_{10})$ is the effective reflection coefficient, and $k=2\pi/\lambda$ is the wave number of the incident radiation (all further calculations are done for $\lambda=3$ cm). The function $G(\mathbf{r})$ specifies the amplitude distribution of the incident field over the scattering area S and for $y_0=0$ has the following form [15]:

$$G(\mathbf{r})=\exp\left[-1.38\left(\frac{(x-x_0)^2\,\cos^2\theta_0}{R_0^2\delta_x^2}+\frac{y^2}{R_0^2\delta_y^2}\right)\right]. \tag{2}$$

The correlation function of the reflected electromagnetic field is found from the formula $K_{\mathrm{m}}(\tau)=\langle E_{\mathrm{m}2}E_{\mathrm{m}1}^*\rangle$, where the asterisk denotes complex conjugation and the angle brackets, statistical averaging over the scattering surface. Algebra is given in detail in the Appendix.

For further algebra, we use the approach employed in [18]. As a result, we arrive at formulas for the shift of the reflected signal f_{sh} with respect to the carrier frequency and the width Δf_{10} of the Doppler spectrum at the level -10 dB with respect to the maximum:

$$\begin{aligned}f_{\mathrm{sh}}=\frac{1}{\lambda}\bigg[&2V\sin\varphi_0\sin\theta_0\cos\beta-\frac{2V\sin\beta}{\cos\theta_0}-\frac{2K_{xt}\cos\varphi_0\sin\theta_0}{\sigma_{xx}^2}\\&-\frac{\alpha_p\alpha_y\sigma_{xx}^2\sin\theta_0}{2\alpha_n}+\frac{R_{xx}^2\alpha_u\alpha_0\alpha_n\delta\,\cos^2\theta_0\,\mathrm{tg}\,\theta_0}{4\alpha_e}-\frac{\alpha_s\alpha_z\delta\,\mathrm{tg}\,\theta_0}{2\Delta_{ay}\alpha_r}\bigg],\end{aligned} \tag{3}$$

$$\Delta f_{10}=\frac{4\sqrt{\ln 10}}{\lambda}\left[\frac{2\alpha_t\cos^2\theta_0}{\sigma_{xx}^2}-\frac{\alpha_p^2\sigma_{xx}^2\cos^2\theta_0}{2\alpha_n}+\frac{R_{xx}^2\alpha_n\alpha_u^2\delta\,\cos^2\theta_0}{4\alpha_e}+\frac{\alpha_s^2\delta}{4\Delta_{ay}\alpha_r}\right]^{1/2}. \tag{4}$$

The coefficients in Eqs. (3) and (4) are given in the Appendix.

Figure 2 shows the Doppler spectra for different wind velocities in the case of a fixed radar. Calculations are done for the following conditions: the antenna slewing angle and the roughness propagation direction amount to 0 and 180°, respectively, the incidence angle $\theta_0=5°$, the beam width $\delta_x=\delta_y=1°$, and the wind velocities are 5, 10, and 15 m/s.

Here, the Doppler spectrum shift means the frequency shift of the power spectral density maximum of the reflected signal with respect to the carrier frequency. We determine the DS width at the power level -10 dB with respect to the maximum (see Fig. 2).

2.1. Influence of the sensing parameters on the DS shift and width

We studied the dependences of the shift and width of the Doppler spectrum on different parameters. The main properties of the DS for a narrow-beam antenna in the case of a fixed carrier are well known: with increase in the wind velocity, the shift and width of the DS also increase. An increase in the incidence angle leads to an increase in the shift and a decrease in the width of the DS. As an example, Fig. 3 shows the dependence of the DS shift and width on the incidence angle. Calculations were performed for the wind velocity 5 m/s, and the antenna slewing angle and the roughness propagation direction amounted to 0 and 180°, respectively. It appears that the DS width and shift coincide, respectively, for the following antenna parameters: $\delta_x=1°$, $\delta_y=1°$ and $\delta_x=1°$, $\delta_y=20°$ (curves *1* and *3*, respectively), and if the antennas have the following characteristics: $\delta_x=20°$, $\delta_y=1°$ and $\delta_x=20°$, $\delta_y=20°$(curves *2* and *4*, respectively). This is related to the combined effect of the anisotropy of sea-surface roughness and the anisotropy of the antenna.

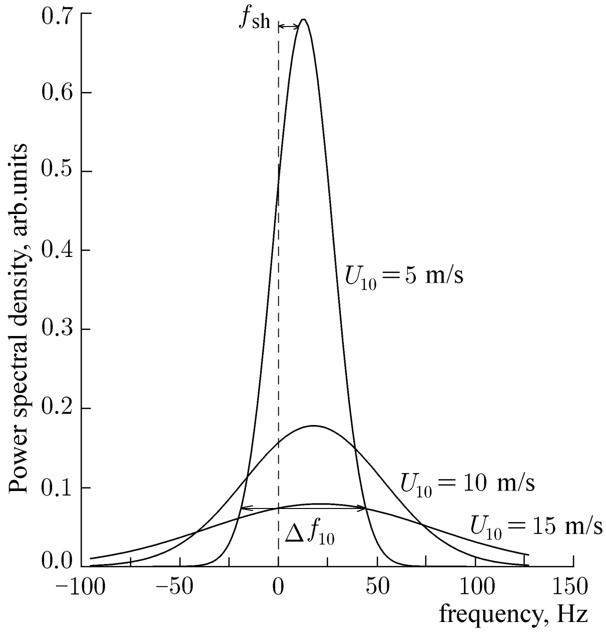

Fig. 2.

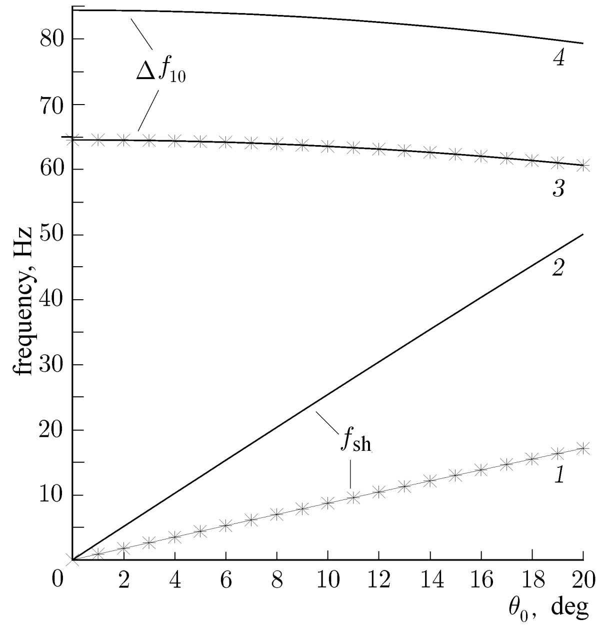

Fig. 3.

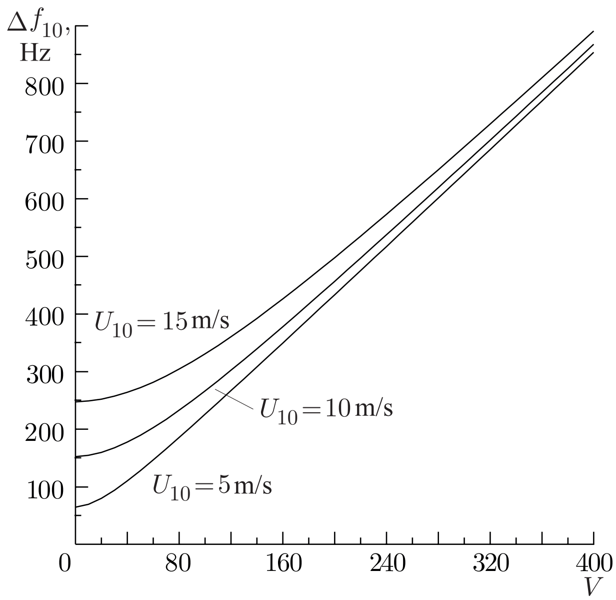

Fig. 4.

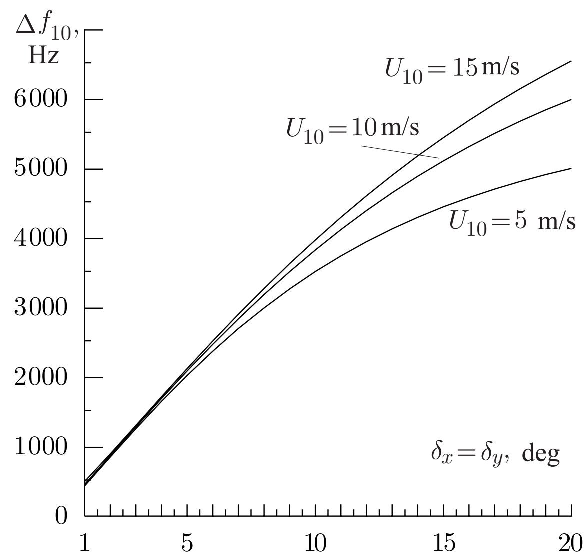

Fig. 5.

The motion (velocity) of a radar does not affect the power of the reflected electromagnetic signal. This explains why the use of the backscattering cross section for interpreting the remote-sensing results is attractive compared with the DS of the reflected electromagnetic signal.

Consider the influence of the radar velocity on the width and shift of the DS. Figure 4 shows the dependence of the DS width on the carrier velocity. Calculations were performed for the following conditions: the radar moves upwind toward the roughness, the antenna slewing angle $\varphi_0 = 0$, the incidence angle $\theta_0 = 5°$, the beamwidth $\delta_x = \delta_y = 1°$, and the wind velocity was chosen equal to 5, 10, and 15 m/s.

As is seen in Fig. 4, the DS width for a fixed radar is considerably dependent on the wind velocity. To be more precise, wind generates sea-surface roughness, and the DS width depends on the orbital-velocity variance. However, as the carrier velocity increases, the curves corresponding to different values of U_{10} become closer to each other, i. e., the DS width ceases to depend on the wind velocity. This is related to the fact that the orbital velocities are much smaller than the airplane velocity, i. e., their contribution is only a small correction which decreases with decrease in the carrier velocity. This feature precluded the use of the DS for solving the problems of radar sensing from a moving carrier since in the case of a narrow beam, only the velocity of the carrier itself can be retrieved (see Fig. 4).

However, this problem has a solution. The point is that the Doppler spectrum width in the case of a moving carrier depends on both the antenna beamwidth and the surface-roughness parameters. This effect can be used for determining the scattering-surface parameters.

Consider the influence of the beamwidth on the shift and width of the Doppler spectrum. Figure 5 shows the dependence of the DS width on the beamwidth for a moving carrier. Calculations were performed for the following conditions: the radar moves upwind toward the roughness, the carrier velocity is 200 m/s, the incidence angle $\theta_0 = 5°$, the beamwidth $\delta_x = \delta_y$ is varied from $1°$ to $20°$, and the wind velocity is equal to 5, 10, and 15 m/s.

It is seen in Fig. 5 that the beamwidth of the Doppler spectrum is only weakly dependent on the wind velocity, in agreement which the conclusion, which follows from Fig. 4, that the radar does not "see" the surface. As the beamwidth becomes greater, the curves in Fig. 5 diverge, i. e., the DS begins to depend on the roughness parameters, and the radar begins to "see" the surface.

To explain this effect, we address Fig. 6 showing the cases of weak (Fig. 6*a*) and strong (Fig. 6*b*) roughness where a wide-beam antenna is used.

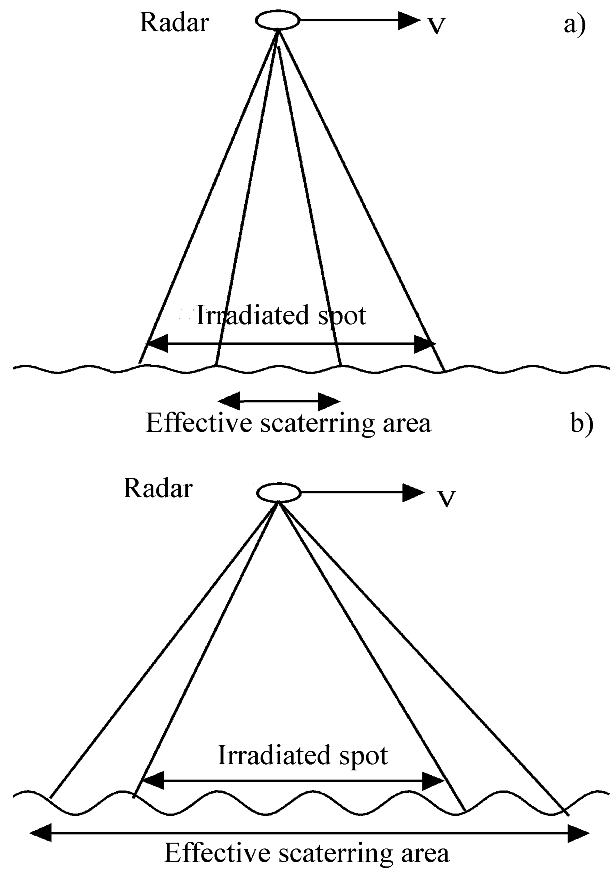

Fig. 6.

It is known that at small incidence angles, the backscattering occurs on the surface areas oriented perpendicular to the incident radiation. The presence of such areas gives rise to the reflected signal (quasi-mirror component). The greater the surface-slope variance, the broader the quasi-mirror scattering area since scattering areas with large sloping angles exist in this case.

When the sea surface is irradiated by a wide-beam radar, the reflected signal can be "picked up" not from the entire irradiated spot, but from the effective scattering area. The size of the effective scattering surface depends on the variance of the slopes determining the area from which the reflected signal can be received. We call this area the effective scattering area. If the size of the irradiated spot is smaller than the effective scattering area, then the reflected singal is contributed by the entire irradiated surface (as, e. g., in the case of a narrow-beam antenna and strong roughness). If the effective scattering surface is smaller than the irradiated spot, then the reflected signal arrives not from the whole irradiated spot, but only from the effective scattering area (as, e. g., in the case of a wide-beam antenna and weak roughness). The surface-slope variance depends on the wind velocity, and, therefore, the higher the wind velocity, the larger the effective scattering area.

For a narrow-beam antenna (e. g., for $\delta_x = \delta_y = 1°$), the irradiated spot is smaller than the effective scattering area for all wind velocities. Hence, the DS parameters do not depend on the wind velocity in the case of a narrow-beam antenna for a moving carrier (see Fig. 5). In the case of a wide-beam antenna, the irradiated spot turns out to be larger than the effective scattering area, and, therefore, the DS width is dependent on the wind velocity, as follows from Fig. 5.

Thus, in the case of a narrow-beam antenna, the spot from which the reflected signal comes is smaller than the effective scattering area, and the reflected signal is collected from the entire irradiated surface for

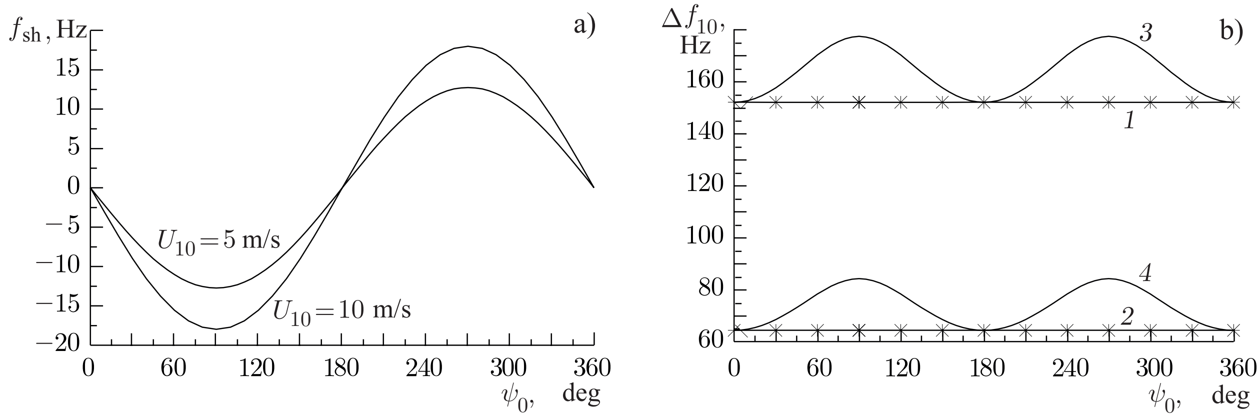

Fig. 7.

any wind velocity. By increasing the antenna beamwidth, we make the effective scattering area dependent on the wind velocity. Hence, the influence of the wind velocity on the DS characteristics is observed in the latter case.

Below we consider the methods for determining the scattering-surface characteristics by the Doppler spectrum.

2.2. Method for measurement of the surface-slope variance and the roughness propagation direction

A study of the DS properties made it possible to propose an algorithm for measuring the surface-slope variance and the roughness propagation direction from a moving carrier.

Consider the influence of the roughness propagation direction on the DS characteristics in the case of a fixed carrier. Figure 7 shows the dependence of the shift (Fig. 7*a*) and width (Fig. 7*b*) of the Doppler spectrum on the roughness propagation direction for a fixed radar. Calculations were performed for the following conditions: the beamwidth $\delta_x = \delta_y = 1°$, the beam slewing angle $\varphi_0 = 90°$, the incidence angle $\theta_0 = 5°$, and the wind velocities $U_{10} = 5$ and 10 m/s. The DS shift has the minimum value when the roughness propagation direction coincides with the slewing angle of the antenna, is equal to zero when the roughness propagates perpendicular to the slewing angle of the antenna, and reaches the maximum when the antenna radiates in the direction opposite to the roughness propagation direction.

In Fig. 7*b*, curve *1* (wind velocity 10 m/s) and curve *2* (wind velocity 5 m/s) correspond to the case of a narrow beam pattern, and curve *3* (wind velocity 10 m/s) and curve *4* (wind velocity 5 m/s) correspond to a knife-edge beam pattern (wide and narrow in two mutually perpendicular directions, $\delta_x = 1°$ and $\delta_y = 20°$). In the case of a narrow-beam antenna, the width of the Doppler spectrum does not depend on the roughness propagation direction since it is determined by the vertical component of the orbital velocity (curves *1* and *2*).

To distinguish the roughness propagation direction, we choose a knife-beam antenna, i. e., specify the BP asymmetry, and determine the surface-roughness asymmetry. As is seen in Fig. 7*b*, the DS width is minimum if the antenna beam is perpendicular to the roughness propagation direction and is maximum if these directions are collinear (curves *3* and *4*). Hence, the roughness propagation direction can be determined from the spectrum width.

We now describe the method for determining the roughness propagation direction from a moving carrier, e. g., an airplane.

The first measurements are performed from an airplane carrying out a circular flight with the BP oriented along the flight direction. This permits one to determine the roughness propagation direction. Figure 8 shows the dependence of the DS width for a circular flight (the carrier velocity $V = 200$ m/s, the

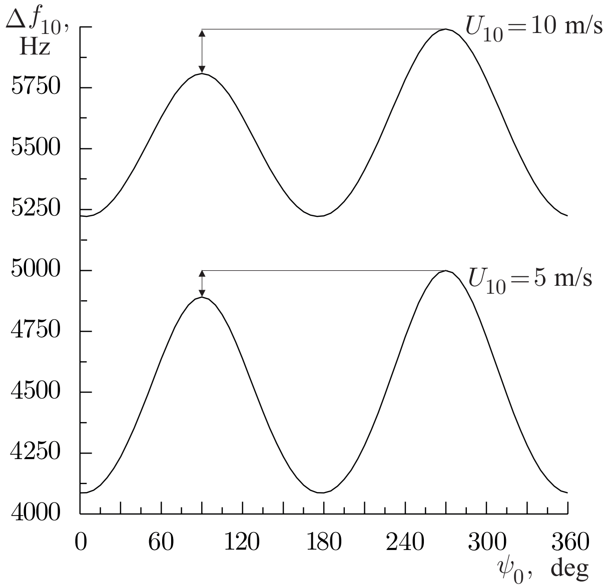

Fig. 8.

antenna slewing angle $\varphi_0 = 90°$, and the beamwidth is given by $\delta_x = 20°$ and $\delta_y = 1°$). The obtained dependence has two maxima, different in magnitude, by which the roughness propagation direction can be retrieved. The smaller maximum corresponds to the case where the radar moves in the roughness propagation direction and the larger maximum, the case where the radar moves in the opposite direction. This is explained by the fact that the radar velocity is added to the phase velocity of the wave when the airplane moves opposite to the roughness propagation direction and is subtracted when the airplane moves in the roughness propagation direction. Thus, by the DS width, one can determine unambiguously the direction of roughness propagation. Then the airplane moves in parallel to the roughness propagation direction and the subsequent measurements of the DS shift and width are performed for two BP orientations — along and across the carrier motion.

The question arises: "Is it possible to measure the angle β for taking into account variations in the flight altitude with respect to the scattering surface and will the flight-altitude variation impair the accuracy of measurement of the characteristics of the surface itself?" Let the BP be oriented along the radar motion, i. e., let the antenna slewing angle $\varphi_0 = 90°$. Since the motion is along the roughness propagation direction ($\psi_0 = 90°$), the correlation coefficients $K_{xy} = K_{xt} = 0$. Taking what was said above into account, from Eqs. (3) and (4) we obtain the following expressions for the shift and width of the Doppler spectrum:

$$f_{\rm sh}^{(1)} = \frac{1}{\lambda}\left[2V\sin\theta_0\cos\beta - \frac{2K_{yt}\sin\theta_0}{\sigma_{yy}^2} - \frac{2V\sin\beta}{\cos\theta_0} - \left(\frac{2K_{yt}}{\sigma_{yy}^2} - 2V\cos\beta\right)\frac{\delta_x^2\sin\theta_0}{5.52\sigma_{yy}^2+\delta_x^2}\right], \tag{5}$$

$$\Delta f_{10}^{(1)} = \frac{4\sqrt{\ln 10}}{\lambda}\left[2\sigma_{tt}^2\cos^2\theta_0 - \frac{2K_{yt}^2}{\sigma_{yy}^2}\cos^2\theta_0 + 2\cos^2\theta_0\left(\frac{K_{yt}}{\sigma_{yy}^2} - V\cos\beta\right)^2\frac{\sigma_{yy}^2\delta_x^2}{5.52\sigma_{yy}^2+\delta_x^2}\right]^{1/2}. \tag{6}$$

Let us change the antenna orientation, putting $\varphi_0 = 0$ and retaining the motion direction (roughness propagation direction $\psi_0 = 90°$). In this case, the correlation coefficients $K_{xy} = K_{xt} = 0$. With allowance for these assumptions, from Eq. (5) we obtain the following expressions for the shift and width of the Doppler spectrum:

$$f_{\rm sh}^{(2)} = -\frac{2V\sin\beta}{\lambda\cos\theta_0}, \tag{7}$$

$$\Delta f_{10}^{(2)} = \frac{4\sqrt{\ln 10}}{\lambda}\left[2\cos^2\theta_0\left(\sigma_{tt}^2 - \frac{K_{yt}^2}{\sigma_{yy}^2}\right) + 2\left(\frac{K_{yt}}{\sigma_{yy}^2} - V\cos\beta\right)^2\frac{\sigma_{yy}^2\delta_y^2\cos^2\theta_0}{5.52\sigma_{yy}^2\cos^2\theta_0+\delta_y^2}\right]^{1/2}. \tag{8}$$

From Eq. (7), it is easy to find the angle β which determines variations in the radar altitude above the sounded surface.

Using the obtained equations and bearing in mind that $\delta_x = 1°$ and $\delta_y = 20°$, from Eqs. (5)–(8) one can express the following sea-surface characteristics: the sea-slope variance, the orbital-velocity variance, and the coefficient of cross correlation between slopes and the vertical component of the orbital velocity.

Variation in the radar altitude above the sounded surface is specified by the angle β which can be determined using the formula $\beta = -\arcsin[f_{\rm sh}^{(2)}\lambda\cos\theta_0/(2V)]$, where $f_{\rm sh}^{(2)}$ is the DS shift corresponding to the case where the BP is oriented perpendicular to the direction of radar motion (see Eq. (7)).

In what follows we give the formulas for calculating the variance of sea-surface slopes along the direction of carrier motion:

$$\sigma_{yy}^2 = \frac{2\left(f_{\text{sh}}^{(1)} + \dfrac{2V\sin\beta}{\lambda\cos\theta_0}\right)^2 \delta_x^2\lambda^2\cos^2\theta_0\,(\delta_y^2 - \delta_x^2\cos^2\theta_0) - 22.08\,(A_2^2 - A_1^2)\,\delta_y^2\sin^2\theta_0}{(A_2^2 - A_1^2)\,11.04^2\sin^2\theta_0\cos^2\theta_0 - \left(f_{\text{sh}}^{(1)} + \dfrac{2V\sin\beta}{\lambda\cos\theta_0}\right)^2 11.04\lambda^2\cos^2\theta_0\,(\delta_y^2 - \delta_x^2\cos^2\theta_0)}\,, \tag{9}$$

where

$$A_2 = \frac{\lambda\,\Delta f_{10}^{(2)}}{4\sqrt{\ln 10}}\,, \qquad A_1 = \frac{\lambda\,\Delta f_{10}^{(1)}}{4\sqrt{\ln 10}}\,.$$

Then we write the expressions for the orbital-velocity variance obtained from Eqs. (6) and (8), respectively:

$$\sigma_{tt}^2 = \frac{A_1^2}{2\cos^2\theta_0} + \frac{K_{yt}^2}{\sigma_{yy}^2} - \left(\frac{K_{yt}}{\sigma_{yy}^2} - V\cos\beta\right)^2 \frac{\delta_x^2\sigma_{yy}^2}{5.52\sigma_{yy}^2 + \delta_x^2}\,, \tag{10}$$

$$\sigma_{tt}^2 = \frac{A_2^2}{2\cos^2\theta_0} + \frac{K_{yt}^2}{\sigma_{yy}^2} - \left(\frac{K_{yt}}{\sigma_{yy}^2} - V\cos\beta\right)^2 \frac{\delta_y^2\sigma_{yy}^2}{5.52\sigma_{yy}^2\cos\theta_0 + \delta_y^2}\,. \tag{11}$$

In what follows we present the formulas for the coefficient of cross correlation between the sea-surface slopes and the orbital velocities, which were obtained by two methods. Equation (12) was obtained from Eq. (6), and Eq. (13) was obtained by subtracting the DS width for the antenna oriented perpendicular to the carrier motion (8) from the DS width for the antenna oriented along the radar motion direction (6):

$$K_{yt} = V\sigma_{yy}^2\cos\beta - \left(f_{\text{sh}}^{(1)} + \frac{2V\sin\beta}{\lambda\cos\theta_0}\right)\frac{\lambda\,(5.52\sigma_{yy}^2 + \delta_x^2)}{11.04\sin\theta_0}\,, \tag{12}$$

$$K_{yt} = V\sigma_{yy}^2\cos\beta + \frac{1}{\cos\theta_0}\sqrt{\frac{(A_2^2 - A_1^2)\,(5.52\sigma_{yy}^2\cos^2\theta_0 + \delta_y^2)\,(5.52\sigma_{yy}^2 + \delta_x^2)}{11.04\,(\delta_y^2 - \delta_x^2\cos^2\theta_0)}}\,. \tag{13}$$

Thus, we obtained formulas for calculating the surface-slope variance, the coefficient of cross correlation between the slopes and the orbital velocities, and the orbital-velocity variance.

The orbital velocity variance σ_{tt}^2 and the coefficient K_{yt} of cross correlation between the sea-surface slopes and the vertical component of the orbital velocity are strongly dependent on the carrier velocity fluctuation. Since the carrier velocity is much larger than the phase velocity of the surface wave, moderate fluctuations in V lead to a large error when the orbital-velocity variance is retrieved.

The slope variance in the carrier motion direction is measured with high accuracy, and the slope variance is only slightly affected by such paramters as the carrier-velocity fluctuations and the errors of measurement of the DS shift and width. The slope variance σ_{yy}^2 is more sensitive to fluctuations in the measurement of the incidence angle, but the required accuracy of measurement of σ_{yy}^2 can be reached with increasing incidence angle.

If the error of specifying the carrier velocity is put equal to 10 m/s (5%) for $V = 200$ m/s, then the error of measurement of the slope variance σ_{yy}^2 will not exceed 2%. The error of measurement of the slope variance will not exceed 2% if the DS shift and width are measured with 20% error. If the error of measurement of the incidence angle $\Delta\theta_0$ is equal to 1° for $\theta_0 = 1°$, then the error of measurement of σ_{yy}^2 will amount to about 60%, but as the incidence angle increases to 10° for the same error $\Delta\theta_0 = 1°$, the error of measurement of σ_{yy}^2 decreases to 10%.

We also considered the case where the DS shift and width increased (decreased) by 5% when the antenna was oriented along the direction of carrier motion and decreased (increased) by 5% when the antenna orientation was perpendicular to this direction. In this case, the error of measurement of the slope variance is equal to 15%. Thus, the slope variance can be measured with good accuracy. Knowledge of the slope variance will make it possible to measure the surface-wind velocity more accurately.

Let us write the formulas for determining the phase velocity of the surface wave. It can easily be seen that the coefficient K_{yt}/K_{yy} represents the phase velocity of the roughness [14]. We write the expression for the phase velocity using Eq. (5) for the DS shift:

$$\frac{K_{yt}}{K_{yy}} = 2V\cos\beta - \left(f_{\mathrm{sh}}^{(1)} + \frac{2V\sin\beta}{\lambda\cos\theta_0}\right)\frac{\lambda\,(5.52\sigma_{yy}^2 + \delta_x^2)}{5.52\sigma_{yy}^2\sin\theta_0}\,. \tag{14}$$

The second formula for the phase velocity can be derived as follows.

Equation (8) (the antenna is oriented perpendicular to the airplane flight direction) must be subtracted from Eq. (6) for the DS width (the antenna is oriented along the airplane flight direction), whence

$$\frac{K_{yt}}{K_{yy}} = 2V\cos\beta + \frac{2}{\sigma_{yy}^2\cos\theta_0}\sqrt{\frac{(A_2^2 - A_1^2)\,(5.52\sigma_{yy}^2\cos^2\theta_0 + \delta_y^2)\,(5.52\sigma_{yy}^2 + \delta_x^2)}{11.04\,(\delta_y^2 - \delta_x^2\cos^2\theta_0)}}\,. \tag{15}$$

The third method of measuring the phase velocity is as follows. The direction of roughness propagation is determined from an airplane carrying out a circular flight. Here, the DS shifts are known for the carrier motion along (f_1^+) and across (f_1^-) the direction of roughness propagation. If the DS shifts for two directions are known, then it can easily be seen that $f_{\mathrm{sh}}^{-(1)} - f_{\mathrm{sh}}^{+(1)} = 4V_{\mathrm{ph}}/(\lambda\sin\theta_0)$. Therefore, one can find the average phase velocity V_{ph}. However, it should be mentioned that such an estimate is only valid for a narrow-beam antenna. Knowing the phase velocity, one can find the typical wavelength of the surface wave:

$$L = 2\pi V_{\mathrm{ph}}/g, \tag{16}$$

where g is the free-fall acceleration.

Finally, we outline the results in a systematic way. The measurement procedure is given in the form of a block diagram in Fig. 9. The direction of roughness propagation is determined in the circular flight mode and for a knife-beam antenna oriented along the carrier motion direction. During the further measurements, the carrier moves along the direction of roughness propagation, and the measurements are performed with the antenna oriented along and across the carrier motion. Thus, the DS shift and width are measured for two cases. Using these data, one calculates the slope variance, the phase velocity, and the wavelength of the surface wave.

3. CONCLUSIONS

On the basis of the Kirchhoff method of the theory of scattering of an electromagnetic field by a statistically rough surface, we obtained the solution of the problem on the Doppler spectrum of a microwave radar signal reflected from a sea surface at small incidence angles. The new model was developed with allowance for the influence of the beam width on the reflected-signal characteristics. The variation in the carrier flight altitude during measurements was taken into account for the first time. The dependences of the DS shift and width on the beamwidth, the antenna orientation, and other sensing parameters were studied. It is shown that not only the carrier velocity can be measured from a moving carrier using a narrow-beam

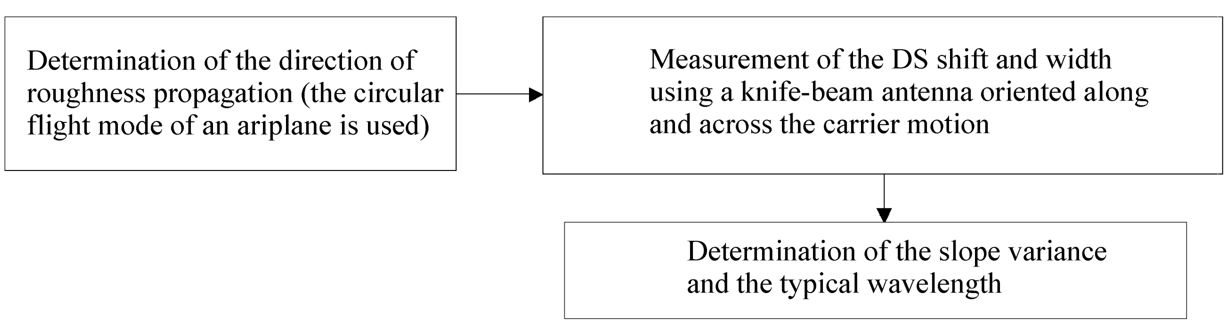

Fig. 9.

antenna, but also the scattering-surface characteristics can be measured in such a way using a knife-beam antenna. As a result of the theoretical study, we developed a new algorithm for airborne measurement of the direction of roughness propagation, the surface-slope variance, and the typical wavelength.

This work was supported by the Russian Foundation for Basic Research (project No. 03–05–64259) and the Council for Support of the Leading Scientific Schools of the Russian Federation (project No. NSh–1637.2003.2)

APPENDIX

Within the Kirchhoff-method approximation, the complex amplitude of the scattered field of the quasi-mirror component is given by [14–17]

$$E_m(t) = \frac{F_{\text{eff}}(U_{10}) E_0 k}{2\pi i \cos\theta_0 R_0} \int\limits_S G(\mathbf{r}) \exp(-2ikR_1)\,\mathrm{d}S, \tag{A1}$$

where E_0 is the amplitude of the incident field near the scattering surface, U_{10} is the wind velocity at the height 10 m above the surface, $F_{\text{eff}}(U_{10})$ is the effective reflection coefficient, $k = 2\pi/\lambda$ is the wave number of the incident radiation, θ_0 is the incidence angle, and R_0 and R_1 are the oblique distances to the scattering-area center and to the current reflection point, respectively.

The function $G(\mathbf{r})$ specifies the amplitude distribution of the incident field over the scattering area S and has the following form [15]:

$$G(\mathbf{r}) = \exp\left[-1.38\left(\frac{(x-x_0)^2\ \cos^2\theta_0\cos^2\varphi_0}{R_0^2\delta_x^2} + \frac{(y-y_0)^2\cos^2\theta_0\sin^2\varphi_0}{R_0^2\delta_y^2}\right)\right]. \tag{A2}$$

The correlation function of the reflected electromagnetic field is given by the well-known formula $K_{\mathrm{m}}(\tau) = \langle E_{\mathrm{m}2}E_{\mathrm{m}1}^*\rangle$, where the asterisk denotes complex conjugation and the angle brackets, statistical averaging over the scattering surface.

For further algebra, we expand R_1 in a series in the vicinity of R_0, i. e.,

$$\begin{aligned} R_1 = \sqrt{x_1^2 + (y_1 + Vt\cos\beta)^2 + (\zeta_1 - H_0 - Vt\sin\beta)^2} &\approx R_0 + R'_x\,(x_1-x_0) + R'_y\,(y_1-y_0) + R'_z\zeta_1 \\ &+ R''_{xx}\,(x_1-x_0)^2/2 + R''_{yy}\,(y_1-y_0)^2/2 + R''_{xy}\,(x_1-x_0)\,(y_1-y_0) \\ &\approx R_0 + (x_1-x_0)\cos\psi_0\sin\theta_0 + (y_1-y_0)\sin\psi_0\sin\theta_0 - \zeta_1\cos\theta_0 \\ &+ \frac{1-\cos^2\psi_0\sin^2\theta_0}{R_0}\,(x_1-x_0)^2 + \frac{1-\sin^2\psi_0\sin^2\theta_0}{R_0}\,(y_1-y_0)^2, \end{aligned}$$

where the factors of the form R'_α and $R''_{\alpha\beta}$ denote partial derivatives of R with respect to the variables $\alpha \in \{x, y, z\}$ and $\beta \in \{x, y\}$.

We denote the distance to the scattering-area center at successive instants of time t and $t+\tau$ as R_1 and R_2. Then $R_1(t) = R_0(t)$ and $R_2(t+\tau) = R_0(t) + Vt\sin(\beta)/\cos(\theta_0)$.

Under the above assumptions, the expression for the correlation function of the reflected field can be written as

$$K_m(\tau) = \frac{|F_{\text{eff}}(U_{10})|^2\,E_0^2k^2}{4\pi^2R_0^2\cos^2\theta_0}\left\langle \iint\limits_{S_1\,S_2} G(\mathbf{R}_1)G(\mathbf{R}_2)\exp(-2ikR_2)\exp(2ikR_1)\,\mathrm{d}S_1\,\mathrm{d}S_2\right\rangle. \tag{A3}$$

Next we find the product $G(\mathbf{R}_1)G(\mathbf{R}_2)$. Using simple algebra and neglecting small terms of order higher than second, we obtain

$$G(\mathbf{R}_1)G(\mathbf{R}_2) \approx \exp[-(a_xx^2 + a_yy^2 + 2xya_{xy} + V^2t^2a_y\cos^2\beta)], \tag{A4}$$

where

$$a_x = \Delta_x \cos^2 \varphi_0 + \Delta_y \sin^2 \varphi_0, \qquad a_y = \Delta_x \sin^2 \varphi_0 + \Delta_y \cos^2 \varphi_0, \qquad a_{xy} = (\Delta_x - \Delta_y) \cos \varphi_0 \sin \varphi_0,$$

$$\Delta_x = \frac{2.76 \cos^2 \theta_0}{R^2 \delta_x^2}\,, \qquad \Delta_y = \frac{2.76}{R_0^2 \delta_y^2}\,.$$

Let us substitute Eq. (A4) into Eq. (A3) and average over a large-scale surface ζ (see [14]). Finally, we obtain the following expression for the correlation function $K_m(\tau)$:

$$K_m(\tau) = \frac{|F_{\text{eff}}(U_{10})|^2}{2\cos^4\theta_0 \sqrt{\alpha_n a_x^0 a_y^0 \alpha_\nu \alpha_r}} \exp\left[-\frac{\text{tg}^2\,\theta_0}{\alpha_n} \left(|K_{yy}|\,\cos^2\varphi_0 + |K_{xx}|\,\sin^2\varphi_0 + K_{xy}\cos\varphi_0\sin\varphi_0\right)\right]$$

$$\times\, \exp\left[\frac{\text{tg}^2\,\theta_0}{4} \left(\frac{R_{xx}^2 \alpha_0^2}{4R_0^2 a_x^0\,\Delta_x\,\alpha_\nu} + \frac{\alpha_z^2}{R_0^2 a_y^0\,\Delta_y\,\alpha_r}\right)\right] \exp[-i\tau k \omega_{\text{t}}]\, \exp[-\tau^2 k^2 \omega_{\text{s}}], \tag{A5}$$

where

$$\omega_{\text{t}} = -2V\sin\varphi_0\sin\theta_0\cos\beta + \frac{2V\sin\beta}{\cos\theta_0} - \frac{K_{xt}\cos\varphi_0\sin\theta_0}{|K_{xx}|}$$
$$+\, \frac{\alpha_p\alpha_y\,|K_{xx}|\,\sin\theta_0}{\alpha_n} - \frac{R_{xx}^2\alpha_u\alpha_0\alpha_n\,\delta\cos^2\theta_0\,\text{tg}\,\theta_0}{4\alpha_e} + \frac{\alpha_s\alpha_z\delta\,\text{tg}\,\theta_0}{2\,\Delta_{ay}\,\alpha_r}\,,$$

$$\omega_{\text{s}} = \frac{\alpha_t\cos^2\theta_0}{K_{xx}} - \frac{|K_{xx}|\,\alpha_p^2\cos^2\theta_0}{\alpha_n} + \frac{R_{xx}^2\alpha_n\alpha_u^2\delta\cos^2\theta_0}{4\alpha_e} + \frac{\alpha_s^2\delta}{4\,\Delta_{ay}\,\alpha_r}\,;$$

$$\alpha_n = 4\,|K_{xx}|\,|K_{yy}| - K_{xy}^2\,, \qquad \alpha_t = 4\,|K_{tt}|\,|K_{xx}| - K_{xt}^2\,,$$

$$a_x^0 = \cos^2\varphi_0 + \frac{\Delta_y}{\Delta_x}\,\sin^2\varphi_0, \qquad a_y^0 = \cos^2\varphi_0 + \frac{\Delta_x}{\Delta_y}\,\sin^2\varphi_0,$$

$$\alpha_\nu = 1 + \frac{R_{xx}^2\,|K_{yy}|}{R_0^2\,\Delta_x\,a_x^0\alpha_n\cos^2\theta_0}\,, \qquad a_y = 2\sin\varphi_0 + \frac{K_{xy}\cos\varphi_0}{|K_{xx}|}\,, \qquad \alpha_0 = \frac{\cos\varphi_0}{|K_{xx}|\,\cos\theta_0} + \frac{\alpha_y K_{xy}}{\alpha_n\cos\theta_0}\,,$$

$$\alpha_p = 2K_{yt} + \frac{K_{xy}K_{xt}}{|K_{xx}|}\,, \qquad \alpha_u = \frac{K_{xt}}{|K_{xx}|} + \frac{\alpha_p K_{xy}}{\alpha_n}\,,$$

$$R_{yy} = 1 - \sin^2\varphi_0\sin^2\theta_0, \qquad R_{xx} = 1 - \cos^2\varphi_0\sin^2\theta_0, \qquad a_{xy} = 2.76\,(\delta_y^2\cos^2\theta_0 - \delta_x^2), \qquad \delta = \delta_x^2\delta_y^2,$$

$$\Delta_{ay} = 2.76\,(\delta_y^2\sin^2\varphi_0\cos^2\theta_0 + \delta_x^2\cos^2\varphi_0), \qquad \Delta_{ax} = 2.76\,(\delta_y^2\cos^2\varphi_0\cos^2\theta_0 + \delta_x^2\sin^2\varphi_0),$$

$$\alpha_g = 2a_{xy}\alpha_n\cos^2\theta_0\cos\varphi_0\sin\varphi_0 + R_{xx}R_{yy}K_{xy}\delta, \qquad \alpha_e = \Delta_{ax}\alpha_n\cos^2\theta_0 + R_{xx}^2\,|K_{yy}|\,\delta,$$

$$\alpha_s = 2R_{yy}\left(\frac{\alpha_p\,|K_{xx}|}{\alpha_n} - V\cos\beta\right) - \frac{R_{xx}\alpha_u\alpha_g}{2\alpha_e}\,, \qquad \alpha_z = \frac{R_{xx}\alpha_0\alpha_g}{4\alpha_e} - \frac{\alpha_y R_{yy}\,|K_{xx}|}{\alpha_n\cos\theta_0}\,,$$

$$\alpha_r = 1 + \frac{R_{yy}^2\,|K_{xx}|\,\delta}{\Delta_{ay}\,\alpha_n\cos^2\theta_0} - \frac{\alpha_g^2}{4\,\Delta_{ay}\,\alpha_n\alpha_e\cos^2\theta_0}\,.$$

Then we make use of the well-known Wiener–Khinchin relationship between the correlation function $K_m(\tau)$ and the spectrum $S_m(\omega)$ (see [18]):

$$S_m(\omega) = \int K_m(\tau)\exp(-i\omega\tau)\,\mathrm{d}\tau.$$

As a result, the final formula for $S_m(\omega)$ has the form

$$S_m(\omega) = \frac{|F_{\text{eff}}(U_{10})|^2}{2\cos^4\theta_0\,\sqrt{\alpha_n a_x a_y \alpha_\nu \alpha_r}}\sqrt{\frac{\pi}{k^2\omega_{\text{s}}}}\,\exp\left[-\frac{\operatorname{tg}^2\theta_0}{\alpha_n}\left(|K_{yy}|\,\cos^2\varphi_0 + |K_{xx}|\,\sin^2\varphi_0 + K_{xy}\cos\varphi_0\sin\varphi_0\right)\right]$$

$$\times\exp\left[\frac{\operatorname{tg}^2\theta_0}{4}\left(\frac{R_{xx}^2\alpha_0^2}{4R_0^2 a_x^0\,\Delta_x\,\alpha_\nu} + \frac{\alpha_z^2}{R_0^2 a_y^0\,\Delta_y\,\alpha_r}\right)\right]\exp\left[-\frac{(k\omega_{\text{t}}-\omega)^2}{4k^2\omega_{\text{s}}}\right]. \tag{A6}$$

Hence, the Doppler spectrum shift is equal to $f_{\text{sh}} = \omega_{\text{sh}}/(2\pi) = -k\omega_{\text{t}}/(2\pi) = -\omega_{\text{t}}/\lambda$. Then we determine the Doppler spectrum width $\Delta f_{10} = \Delta\omega/(2\pi)$ at the level -10 dB with respect to the maximum: $\exp[-(\Delta\omega)^2/(4k^2\omega_{\text{s}})] = 0.1$, whence $\Delta f_{10} = 2\sqrt{w_{\text{s}}\,\ln 10}\,/\lambda$.

Omitting algebra, we present the final formula for the shift of the reflected signal f_{sh} with respect to the carrier frequency and the Doppler spectrum width Δf_{10} at the level -10 dB with respect to the maximum:

$$f_{\text{sh}} = \frac{1}{\lambda}\left[2V\sin\varphi_0\sin\theta_0\cos\beta - \frac{2V\sin\beta}{\cos\theta_0} - \frac{K_{xt}\cos\varphi_0\sin\theta_0}{|K_{xx}|} - \frac{\alpha_p\alpha_y\,|K_{xx}|\,\sin\theta_0}{\alpha_n} + \frac{R_{xx}^2\alpha_u\alpha_0\alpha_n\delta\cos^2\theta_0\operatorname{tg}\theta_0}{4\alpha_e} - \frac{\alpha_s\alpha_z\delta\operatorname{tg}\theta_0}{2\,\Delta_{ay}\,\alpha_r}\right], \tag{A7}$$

$$\Delta f_{10} = \frac{4\sqrt{\ln 10}}{\lambda}\left[\frac{\alpha_t\cos^2\theta_0}{K_{xx}} - \frac{\alpha_p^2\,|K_{xx}|\,\cos^2\theta_0}{\alpha_n} + \frac{R_{xx}^2\alpha_n\alpha_u^2\delta\cos^2\theta_0}{4\alpha_e} + \frac{\alpha_s^2\delta}{4\,\Delta_{ay}\,\alpha_r}\right]^{1/2}. \tag{A8}$$

The series expansion coefficients of the correlation function of large-scale roughness heights $K(\boldsymbol{\rho},\tau)$ are calculated as follows:

$$K_{\alpha\alpha} = \left.\frac{\partial^2 K(\boldsymbol{\rho},\tau)}{2\,\partial\alpha^2}\right|_{\substack{\rho=0\\ \tau=0}}, \qquad K_{\alpha\beta} = \left.\frac{\partial^2 K(\boldsymbol{\rho},\tau)}{\partial\alpha\,\partial\beta}\right|_{\substack{\rho=0\\ \tau=0\\ \alpha\neq\beta}},$$

where α and β take the values x and y. The coefficients $K_{\alpha\alpha}$ and $K_{\alpha\beta}$ are calculated using the well-known relationship between the correlation function and the roughness spectrum [14, 19, 20], and the variance $\sigma_{\alpha\alpha}^2$ is equal to $2\,|K_{\alpha\alpha}(0,0)|$.

REFERENCES

1. G. S. Brown, *J. Geophys. Res. B*, **84**, No. 8, 2974 (1979).
2. G. S. Brown, H. R. Stanley, and N. A. Roy, *IEEE J. Oceanic Eng.*, No. 6, 59 (1981).
3. D. B. Chelton and P. J. McCabe, *J. Geophys. Res. C*, **90**, 4707 (1985).
4. D. L. Witter and D. B. Chelton, *J. Geophys. Res. C*, **96**, No. 5, 8853 (1995).
5. V. Yu. Karaev, M. B. Kanevsky, G. N. Balandina, and K. Hommenginger, *Issled. Zemli Kosm.*, No. 4, 32 (2002).
6. E. J. Walsh, D. C. Vandermark, C. A. Friehe, et al., *J. Geophys. Res. C*, **103**, No. 6, 12587 (1998).
7. E. J. Walsh, D. W. Hancock, D. E. Hines, et al., *J. Phys. Oceanography*, **15**, 566 (1985).
8. D. D. Crombie, *Nature*, **175**, 681 (1995).
9. C. Ya. Braude, ed., *Radio Oceanographic Studies of Sea-Surface Roughness* [in Russian], Acad. Sci. UkrSSR Press, Kiev (1962).
10. D. E. Barrik, *Boundary-Layer Meteorology*, **13**, 23 (1978).

11. I. M. Fuks, *Sov. Radiophys.*, **9**, 513 (1966).

12. G. R. Valebzuela, *Boundary-Layer Meteorology*, **13**, 61 (1978).

13. M. B. Kanevskii and V. Yu. Karaev, *Radiophys. Quantum Electron.*, **39**, No. 5, 347 (1996).

14. F. G. Bass and I. M. Fuks, *Wave Scattering from Statistically Rough Surfaces*, Pergamon Press, Oxford (1979).

15. S. G. Zubkovich, *Statistical Characteristics of Radio Signals Reflected from a Sea Surface* [in Russian], Sovetskoe Radio, Moscow (1968).

16. G. S. Brown, *IEEE Trans. Antennas Propag.*, **26**, 472 (1968).

17. A. Stogrun, *Radio Sci.*, **2**, No. 4, 415 (1967).

18. V. Yu. Karaev and M. B. Kanevsky, *Issled. Zemli Kosm.*, No. 4, 14 (1999).

19. W. J. Plant and W. C. Keller, *J. Geophys. Res. C*, **95**, No. 9, 16299 (1990).

20. I. M. Fuks, *Akust. Zh.*, **20**, No. 3, 458 (1974).